

Electronic structure of the valence band of the II–VI wide band gap binary/ternary alloy interfaces

D. Olgúin and R. Baquero

Departamento de Física,

Centro de Investigación y de Estudios Avanzados del IPN,

A. P. 14-740, 07000 México D.F.

Abstract

We present an electronic structure calculation of the valence band for some II–VI binary/ternary alloy interfaces. We use the empirical tight-binding method and the surface Green's function matching method. For the ternary alloys we use our previously set Hamiltonians they describe well the band gap change with composition obtained experimentally. At the interface domain, we find three non-dispersive and two interface states besides the known bulk bands. The non-dispersive states are reminiscent of the ones already obtained experimentally as well as theoretically, in (001)–oriented surfaces. We make use of the available theoretical calculations for the (001)–oriented surfaces of the binary compounds and for the binary/binary interfaces to compare our new results with.

PACS: 71.15.Fv, 71.55.Gs, 73.10.-r

I. INTRODUCTION

In recent years, new semiconductor heterostructures have attracted considerable interest. Multiple quantum well structures and superlattices of II–VI compounds are the subject of intensive study because of their interesting optical properties [1–4]. With these structures, energy gaps ranging from the UV to IR are accessible [3–5]. In these systems the binary interfaces are usually lattice mismatched. This lattice mismatch modifies the band alignments, and hence modifies the device optical properties. In searching for the desired material parameters such as band gap, lattice matching to substrates, dielectric contact, carrier mobility, etc., a large number of materials, have been investigated. Recently, high-quality cubic-structured ternary and quaternary alloys have been proposed as appropriate materials for heterostructures [3,4]. Ternary alloys allow a certain control of the induced strain at the interface.

The deep understanding of the physics of the interface is important for the detailed study of thermal, optical, and other properties of quantum-wells and superlattices. The electronic properties at solid–solid interfaces depend sometimes even on details of the interaction between the two atomic layers from the different materials in contact. Our work can be used as a starting point to analyze those details. These are responsible for the characteristics of interface reconstruction, thermodynamic properties, degree of intermixing, stress, compound formation, etc.

In previous work, we have studied the electronic structure of the valence band for the (001)–surface of several II–VI wide band gap semiconductors [6,7], and different binary heterostructures [8]. We have obtained the (001)–projected electronic structure for both, surfaces and binary interfaces using the known Surface Green’s Function Matching (SGFM) method [9].

In the (001)–surfaces in addition to the well known bulk bands and surface resonances, we have described three different structures in the valence band region, the so-called surface induced bulk states (B_h , B_l , and B_s). We have shown that these states owe their origin to the

creation of the surface, that is, they depend on the surface through the boundary condition (the wave function has to be zero at the surface), but they are not surface resonances. They are *surface-induced bulk states* [6,7]. Later we found that this kind of induced states appear at the interface domain as well. Therefore, more generally, we found that any frontier can induce these states. For that reason we have redefined them as frontier-induced semi-infinite medium (FISIM) states since they are not, strictly speaking, *bulk* (infinite medium) states. These FISIM states do not show dispersion as a function of the wave vector \mathbf{k} for the surfaces studied. This is theoretically and experimentally shown for the (001)-oriented CdTe surface [6,7,10,11]. For the binary/binary (001)-oriented II-VI compound interfaces, in contrast, they show some clear dispersion [8].

The interest of the present work is twofold. Firstly, we want to make practical use of our recently set found tight-binding Hamiltonians for the ternary alloys. They reproduce the known experimental change with the composition of the band gap and they can be further used in detailed studies of different physical problems as, for example, the dependence of the transport properties on composition in quantum well structures that avoid stress. The second interest of this work is the study of the evolution of the FISIM states from a non-dispersive character to a dispersive one as stress and different crystal composition enters into play. We show that, if we select a ternary alloy to produce little stress and change only slightly the composition, the FISIM states do exist on both sides of the interface but do not show as much dispersion. So the existence of the FISIM states is due to the existence of a frontier alone and the amount of dispersion is related to the existing stress at the interface and on the chemical character of the interface partner.

We will present in this work the valence band of some II-VI (001)-binary/ternary alloy interfaces and we will concentrate in particular in the FISIM states. The method used is discussed in our previous work. Here we only summarize the relevant features of it in Section II for completeness; Section III is devoted to discuss our results. Finally, we give our conclusions in section IV.

II. THE METHOD

To describe the interface between two semiconductor compounds, we make use of tight-binding Hamiltonians. The Green's function matching method takes into account the perturbation caused by the surface or interface exactly, at least in principle, and we can use the bulk tight-binding parameters (TBP) [12–14]. This does not mean that we are using the same TBP for the surface, or for the interface and the bulk. Their difference is taken into account through the matching of the Green's functions. We use the method in the form cast by García-Moliner and Velasco [9]. They make use of the transfer matrix approach first introduced by Falicov and Yndurain [15]. This approach became very useful due to the quickly converging algorithms of López-Sancho *et al.* [16] Following the suggestions of these authors, the algorithms for all transfer matrices needed to deal with these systems can be found in a straightforward way [17].

The Green's function for the interface, G_I , is given by [9],

$$G_I^{-1} = G_{s(A)}^{-1} + G_{s(B)}^{-1} - I_B H^i I_A - I_A H^i I_B, \quad (1)$$

where $G_{s(A)}$ and $G_{s(B)}$ are the surface Green's function of medium A and B, respectively. $-\mathcal{I}_A H^i \mathcal{I}_B$ and $-\mathcal{I}_B H^i \mathcal{I}_A$ are the Hamiltonian matrices that describe the interaction between the two media. In our model these are 20×20 matrices, the input TBP for these matrices are the average for those of the two media. This is a reasonable approximation when both sides of the interface have the same crystallographic structure and we take the same basis of wave functions.

The tight-binding Hamiltonians for the II–VI ternary alloys are described in detail in Ref. [18]. Briefly speaking, we have used the tight-binding method and, under certain conditions, the virtual crystal approximation to study the ternary alloys. We have included an empirical bowing parameter in the s -on site TBP of the substituted ion. This procedure gave us the correct behaviour of the band gap value with composition [18]. More exactly for the TBP of the ternary alloy, we take

$$\overline{E}_{\alpha,\alpha'}(x) = xE_{\alpha,\alpha'}^{(1)} + (1-x)E_{\alpha,\alpha'}^{(2)}, \quad \alpha, \alpha' = s, p^3, s^* \quad (2)$$

for all but the s -on site TBP of the substituted ion. In eq. (2) $E_{\alpha,\alpha'}^{(1,2)}$ are the TBP for the compound 1 (2); α, α' are the atomic orbitals used in the basis set.

For the s -on site TBP of the substituted ion we use the following expression

$$\overline{E}_{s,\nu}(x, b_\nu) = \overline{E}_{s,\nu}(x) + x(1-x)b_\nu, \quad \nu = a, c \quad (3)$$

where $\overline{E}_{s,\nu}(x)$ is given by eq. (2) and b_ν is the empirical bowing parameter per each different substitution (anion-substitution (a) or cation-one (c)). In Table I we have the empirical bowing parameters used in this work. We do not introduce any further parameter [18].

From the knowledge of the Green's function, the local density of states can be calculated from its imaginary part integrating over the two-dimensional first Brillouin zone, the dispersion relations can be obtained from the poles of the real part. We have applied previously this formalism to surfaces [6,7,12,13], interfaces [8,14,20] and superlattices [21]. Now we present our results.

III. RESULTS AND DISCUSSION

This section is devoted to the discussion of the interface-valence band of the (001)-projected electronic band structure of II-VI binary/ternary alloy interfaces. We will present in this paper the (001)-CdTe/CdSe_{0.15}Te_{0.85}, (001)-CdTe/Zn_{0.17}Cd_{0.83}Te, (001)-ZnSe/ZnSe_{0.87}Te_{0.13}, and (001)-ZnSe/Zn_{0.85}Cd_{0.15}Se interfaces in detail. The interfaces studied have been chosen with a composition (x) as to give a minimum stress. For the lattice parameter value of the materials considered see Table II. As we can see the induced stress is small, about 1%. This magnitude of the induced stress allow us to ignore its effect in our calculation. The real bulk bands as well as the FISIM states, should lie very closely to our calculated ideal case. We adopt the same convention for the interface domain as in Ref. [8]. That is to say, we consider nearest neighbors interactions in our bulk Hamiltonians and, as a consequence, four atomic layers as the interface domain, two belonging to medium A and

two to medium B. To distinguish between the different atomic layers we will call each atomic layer by the medium its neighbors belong to. The atomic layer AA will be the second from the interface into medium A. AB will be the last atomic layer belonging to medium A and facing the first atomic layer of medium B and so on. So the four atomic layers that constitute the interface domain will be labeled AA, AB, BA, and BB. For the interfaces aligned along the (001) direction the two media are facing each other either through its anion or cation atomic layer. In the alloy case, we consider a pseudobinary compound so that the concept of anion and cation atomic layers remain meaningful. We will consider here only anion-anion interfaces but our results can be extended without difficulty to other kind of interfaces. We will project the interface electronic band structure on each atomic layer and we will see how the different states that we found for the free surface and for the binary/binary interface case change or disappear at the binary/ternary one.

It is known that the common anion interfaces have small valence band-offset and the common cation ones have small conduction band-offset, both of the order of some meV [4,5,19]. In consequence, we will use the boundary condition that the top of the valence bands at the interface are aligned and choose this energy as our zero. Accordingly, the conduction band offset will be equal to the difference in the band gaps. The actual calculation of the band offset is still an open theoretical question that we do not want to address in this work [22]. As a general remark, the FISIM states are not Bloch states and therefore the \mathbf{k} -wave number is not expected to be a good quantum number. The existence of a frontier (surface or interface) breaks the symmetry. This does not actually mean that when the Schrödinger equation is solved for different values of \mathbf{k} (the Hamiltonian depends explicitly on it) one should get the same eigenvalue. It is found, theoretically [6,7] as well as experimentally [10,11], that the solution does not depend on \mathbf{k} for the case of a surface. In this case the boundary condition is that the wave function has to be zero at the surface boundary for any value of the derivative. It is the condition for an infinite potential barrier. For the interface it is not so. For the binary/binary case we got a solution that depends on the wave vector, \mathbf{k} , but we should not call it *dispersion* since it is not the behaviour with respect to a quantum

number that we are looking at but rather with respect to a parameter. FISIM states are neither Bloch states nor surface states. They do exist in the semi-infinite medium space but they do not follow the infinite-medium symmetry of the crystal. So we have to look for a different physical reason of their \mathbf{k} -dependence.

The first thing to notice is that the boundary condition is different. For an interface, the wave function has not to be zero, it has to be continuous together with the derivative. The boundary condition therefore will depend on \mathbf{k} . This is because the Hamiltonian describing the interaction depends on it and therefore the wave function that solves the Schrödinger equation does depend on it as well. For this reason its value and its derivative at the border will also depend on it. One does therefore, in general, expect a \mathbf{k} -dependence of the FISIM states eigenvalues for an interface. For a surface the boundary condition is always zero and on the contrary we do not expect a \mathbf{k} -dependence.

In previous work, [8] we have explored the behaviour of the FISIM states at binary/binary interfaces. These represent a strong change at the interface. In this work, we explore the existence and behaviour of the FISIM states at interfaces that do change slowly. Here, ternary alloys are chosen so as to minimize stress (same lattice constant in both sides) and the corresponding binary/ternary alloy interface FISIM states are obtained. Their \mathbf{k} -dependence as expected, is minimum. So, we can conclude that, in general, stress is responsible for the \mathbf{k} -dependence of the FISIM states. This is in agreement with the ideas developed above. Therefore, FISIM states are a consequence of the existence of a frontier and their \mathbf{k} -dependence is a result of the stress at it.

Furthermore, we have obtained from this calculation two interface states in the valence band range for the CdTe-based interfaces and one interface state for the ZnSe-ones. Now we present the details for each interface.

In Figs. 1–4, we show the electronic band structure of the valence band for the interfaces studied here, (001)–CdTe/CdTe_{0.85}Se_{0.15}, (001)–CdTe/Zn_{0.17}Cd_{0.83}Te, (001)–ZnSe/ZnSe_{0.87}Te_{0.13}, and (001)–ZnSe/Zn_{0.85}Cd_{0.15}Se. The dispersion relations are found from the poles (triangles in the figures) of the real part of the interface Green's function. The solid-lines are a guide

to the eye. These are to be compared to the dispersion curves found for the bulk (infinite medium) case. The calculated eigenvalues for the FISIM states are denoted by stars, crosses and points; the dotted lines are intended only as a guide to the eye. We label the FISIM states as B_{Ih} , B_{Il} , and B_{Is} . This convention follows the previous free (001)–surfaces study (see Refs. [6,7]). The energy eigenvalues for all the calculated states are in Tables III and IV.

A. The (001)–CdTe/CdSe_{0.15}Te_{0.85} interface

Fig. 1 shows the projected electronic structure of the valence band for this interface per atomic layer. From the figure is evident that we have obtained the general pattern of the projected band structure of the II–VI semiconductor surfaces [6,7]. As we have commented above we will consider an anion–anion interface and we will align the top of the valence band as our zero of energy. We have obtained that the heavy hole (hh) and light hole (lh) bands show more dispersion in the interface domain than in the semi–infinite medium. They are usually low in energy about 0.7 eV and 0.4 eV, respectively, in all the atomic layers. The spin–orbit band shows almost the same dispersion that in the semi–infinite medium, see Table III.

As is pointed previously [8], the FISIM states B_{Ih} and B_{Il} in the interface domain do not mix with the hh and lh bands, as is observed in the (001)–surface case [6,7], see Fig. 1 and Table IV. The states are lower in energy than the lh band. These upper FISIM states show a slight dependence on \mathbf{k} , but in most of the cases it is less than 0.3 eV. In contrast, the B_{Is} state follows the spin–orbit band as in the semi–infinite medium. In general, from the Fig. 1 we appreciate that the FISIM states show better behaviour than in the binary/binary interfaces [8].

Moreover, in this energy interval we have obtained some states that we identify with *interface states* (IS_1 and IS_2 , the dotted lines in Fig. 1, are a guide to the eye). The first one, at –1.3 eV, in Γ , shows notable dispersion and seems to disappear for \mathbf{k} –values near

the X -point. The second state, with more noticeably dispersion, appears at -1.9 eV in Γ and reaches the X -point in -4.3 eV. However, as we do not know about experimental results in this system we can not give a complete comparison. We only predict the possibility of the existence of these interface states.

B. The (001)–CdTe/Zn_{0.17}Cd_{0.83}Te interface

This system shows almost the same pattern describe above. The calculated valence band electronic structure is presented in Fig. 2. From the Table III we observe that the hh and lh bulk bands show more dispersion than in the semi-infinite medium. In particular the electronic structure projected onto the Cd-atomic layer (Fig. 2a.) shows bigger dispersion for these bands, of about 0.8 and 0.5 eV, respectively, than the semi-infinite medium, see Table III. For the other atomic layers the projected electronic structure shows almost the same pattern all together: the hh and lh bands are 0.5 and 0.3 eV below in energy with respect to the bulk values, respectively. The spin-orbit band, however, in the interface seems to form a barrier of about 0.2 eV from the AA-atomic layer to the BB-atomic layer, see Table III.

In general, the B_{Ih} , B_{Il} and the B_{Is} FISIM states are lower in energy than the hh, lh, and spin-orbit bulk bands, respectively. In the same way that in the previous case, these FISIM states do not mix with the respective bulk bands at X , as in observed in the semi-infinite medium case [6,7]. However, the FISIM states shows slight dependence on \mathbf{k} . As in the previous interface, we obtain two interface states in the present system, label IS_1 and IS_2 in Fig. 2. The IS_1 state, located at -1.3 eV in Γ , shows notable dispersion and reaches the X -point between the hh and lh bulk bands. The IS_2 state, with bigger dispersion than the previous one, is located in Γ at -1.9 eV and reaches the X -point at the same values that the spin-orbit bulk band.

C. The (001)–ZnSe/ZnSe_{.87}Te_{.13} interface

Fig. 3 shows the calculated electronic structure of the valence band for this interface. Opposite to the CdTe-based interfaces, discussed above, the bulk bands and the FISIM calculated states for this system shows almost the same behaviour that in the semi-infinite medium. This observation goes for all the calculated bands but the spin-orbit band in the Γ point, where we obtain, as in the previous case, a discontinuity from the AA-atomic layer to the BB-atomic layer. In this case the spin-orbit band seems to form a potential well, in Γ , of about 0.2 eV, see Table III. On the other hand, for this interface we obtain that the B_{Ih} , B_{Il} , and B_{Is} FISIM states mix with the hh, lh, and spin-orbit bulk bands, respectively, as is observed in the semi-infinite medium [6,7]. In this sense this interface shows better behaviour than the other ones [8]. Although, as previously, we have obtained an interface state for this system, IS_1 . This interface state appears in Γ at -1.7 eV, shows noticeably dispersion and seems to disappear for \mathbf{k} -values near the X -point. However, the state appears notoriously in all the calculated atomic layers.

D. The (001)–ZnSe/Zn_{.85}Cd_{.15}Se interface

Finally, in the Fig. 4 we show our electronic structure calculated for this system. In the same way that the previous case, we obtain that all the calculated states, per atomic layer, for this interface are similar with the semi-infinite medium, see Tables III and IV. In addition to these states, we have an interface state, IS_1 , located in Γ at -1.7 eV and showing notable dispersion. The state do not appear for all the interval between $\Gamma - X$, it seems to disappear for \mathbf{k} -values near the X -point, as we have commented previously for the other interfaces.

IV. CONCLUSIONS

In conclusion, we have calculated the electronic structure of the valence band of the II–VI binary/ternary alloy interfaces. We have used the tight-binding method and the surface Green’s function matching method to obtain the electronic structure projected onto each atomic layer that constitutes the interface domain. For the ternary alloys we have used our tight-binding Hamiltonians described in previous work that give good account for the changes of the band gap with composition as obtained experimentally. Our parametrization includes an empirical bowing parameter for the “ s ” on-site tight-binding parameter of the substituted ion and we use the known virtual crystal approximation for the rest of them. The systems were chosen here so that stress can be ignored for the particular value of the compositional variable. The calculated valence band electronic structure of these interfaces show bulk bands with similar dispersion as for the semi-infinite medium (a system with a surface). The FISIM states observed in the (001)–oriented surfaces and binary/binary interfaces appear also in this case and show an intermediately strong \mathbf{k} –dependence as compare to the previous ones. In the interface domain the calculated states, both the bulk bands and the FISIM states, have a composition that is a combination of the corresponding states of the two media forming the interface.

It is interesting to note further that we have obtained for the binary/ternary alloy case two interface states for the CdTe–based heterostructures and one interface state for the ZnSe–ones that do not show for the binary/binary interfaces at least in the energy interval that we have considered. We will consider the binary/quaternary and the ternary/quaternary alloy interfaces in future work.

REFERENCES

- [1] Tersoff, J.: Phys. Rev. Lett. **52**, 165 (1984)
- [2] Flores F., Tejedor, C.: J. Phys. C. Solid State Phys. **20**, 145 (1987)
- [3] Brasil, M. J. S. P., Tamargo, M. C., Nahory, R. E., Gilchrist, H. L., Martin, R. J.: Appl. Phys. Lett. **59**, 1206 (1991)
- [4] Ichino, K., Iwami, K., Kawakami, Y., Fujita, S. Z., Fujita, S. G.: J. Electronic Mat. **22**, 445 (1993)
- [5] Pelhos, K., Lee, S. A., Rajakarunanayake, Y.: Phys. Rev. B **51**, 13 256 (1995); Rajakarunanayake, Y., Miles, R. H., Wu, G. Y., McGill, T. C.: Phys. Rev. B **37**, 10 212 (1988)
- [6] Olguín, D., Baquero, R.: Phys. Rev. B **50**, 1980 (1994)
- [7] Olguín, D., Baquero, R., Phys. Rev. B **51**, 16 981 (1995)
- [8] Olguín, D., Baquero, R., sent to Phys. Rev. B; cond-mat/9606141.
- [9] García-Moliner, F., Velasco, V. R.: Prog. Surf. Sci. **21**, 93 (1986); Theory of Single and Multiple Interfaces, World Scientific, Singapore, 1992.
- [10] Niles, D., Höchst, H.: Phys. Rev. B **43**, 1492 (1991)
- [11] Gawlik, K. -U., Brüggmann, J., Harm, S., Janowitz, C., Manzke, R., Skibowski, M., Solterbeck, C. -H., Schattke, W., Orlowski, B. A.: Acta Physica Polonica A **82**, 355 (1992)
- [12] Baquero, R., Velasco, V. R., García-Moliner, F.: Physica Scripta **38**, 742 (1988)
- [13] Baquero R., Noguera, A.: Rev. Mex. de Física **35**, 638 (1989)
- [14] Quintanar, C., Baquero, R., García-Moliner, F., Velasco, V. R.: Rev. Mex. de Física **37**, 503 (1991)

- [15] Falicov, L., Yndurain, F.: J. Phys. C: Solid St. Phys. **8**, 147 (1975)
- [16] López-Sancho, M. P., López-Sancho, J. M., Rubio, J.: J. Phys. F: Metal Phys. **14**, 1205 (1984); **15**, 855 (1985)
- [17] Baquero, R.: unpublished
- [18] Olguín, D., de Coss, R., Baquero, R.: to be published.
- [19] Duc, T. M., Hsu, C., Faurie, J. P.: Phys. Rev. Lett. **58**, 1127 (1987)
- [20] Baquero, R., Noguera, A., Camacho, A., Quiroga, L.: Phys. Rev. B **42**, 7006 (1990)
- [21] Velasco, V. R., Baquero, R., Brito-Orta, R. A., García-Moliner, F.: Condens. Matter **1**, 6413 (1989)
- [22] Harrison, W. A., Tersoff, J.: J. Vac. Sci. and Technol. B **4**, 1068 (1986); Cardona, M., Christensen, N. E.: Phys. Rev. B **35**, 6182 (1987); Flores, F., Tejedor, C.: J. Phys. C: Solid State Phys. **20**, 1445 (1987); Kilday, D. G., Margaritondo, G., Ciszek, T. F., Deb, S. K.: J. Vac. Sci. and Technol. B **6**, 1364 (1988); Margaritondo, G.: in *Photoemission and Absorption Spectroscopy of Solids and Interfaces with Synchrotron Radiation*, M. Campagna and R. Rosei edits, Amsterdam, North-Holland, pp. 327, 1990; Priester, C.: J. Phys. III **1**, 481 (1991); Yu, E. T., McCaldin, J. O., McGill, T. C.: Solid State Physics vol. 46, Academic Press., 1992

FIGURES

FIG. 1. Electronic structure of the valence band, per atomic layer, of the (001)–CdTe/CdSe_{0.15}Te_{0.85} interface. The dispersion relations are obtained from the poles (triangles) of the real part of the interface Green’s function. The solid lines are a guide to the eye. B_{Ih} , B_{Il} and B_{Is} are the calculated FISIM states (stars, crosses and points, the dotted lines, intended to show the dispersion, are a guide to the eye). We show the interface states IS_1 and IS_2 .

FIG. 2. Electronic structure of the valence band of the (001)–CdTe/Zn_{0.17}Cd_{0.83}Te interface. See Fig. 1 for details.

FIG. 3. Electronic structure of the valence band of the (001)–ZnSe/ZnSe_{0.87}Te_{0.13} interface. See Fig. 1 for details.

FIG. 4. Electronic structure of the valence band of the (001)–ZnSe/Zn_{0.15}Cd_{0.85}Se interface. See Fig. 1 for details.

TABLES

TABLE I. Empirical bowing parameter for the ternary alloys used in this work. Taken from Ref. [18].

Compound	b_a	b_c
$\text{ZnSe}_{1-x}\text{Te}_x$	-6.964	—
$\text{CdSe}_{1-x}\text{Te}_x$	-0.195	—
$\text{Zn}_{1-x}\text{Cd}_x\text{Se}$	—	0.037
$\text{Zn}_{1-x}\text{Cd}_x\text{Te}$	—	0.020

TABLE II. Lattice parameter ratio for the selected composition and the induced stress for the binary/ternary alloy interfaces studied in the present work.

Interface	Lattice parameter ratio	Induced stress %
$\text{CdTe}/\text{CdSe}_{.15}\text{Te}_{.85}$	6.481/6.4175	1.
$\text{CdTe}/\text{Zn}_{.17}\text{Cd}_{.83}\text{Te}$	6.481/6.4171	1.
$\text{ZnSe}/\text{ZnSe}_{.87}\text{Te}_{.13}$	6.052/5.7239	1.
$\text{ZnSe}/\text{Zn}_{.85}\text{Cd}_{.15}\text{Se}$	5.052/5.7273	1.

TABLE III. Energy-eigenvalues for the heavy hole (hh), light hole (lh), and spin-orbit bands at Γ and X high-symmetry points as obtained for the interface domain for (001)-CdTe/CdSe_{0.15}Te_{0.85}, (001)-CdTe/Zn_{0.17}Cd_{0.83}Te, (001)ZnSe/ZnSe_{0.87}Te_{0.13}, and (001)-ZnSe/Zn_{0.85}Cd_{0.15}Se. The energies are in eV.

		Γ -point	X -point		
System	Atomic layer	E_{so}	E_{hh}	E_{lh}	E_{so}
CdTe / CdSe _{0.15} Te _{0.85}	Cd	-0.8	-2.4	-2.6	-4.2
	Te	-0.8	-2.3	-2.6	-4.2
	Se _{0.15} Te _{0.85}	-0.8	-2.4	-2.6	-4.2
	Cd	-0.8	-2.3	-2.6	-4.2
CdTe / Zn _{0.17} Cd _{0.83} Te	Cd	-1.0	-2.5	-2.7	-4.3
	Te	-0.8	-2.2	-2.5	-4.1
	Te	-0.8	-2.2	-2.5	-4.1
	Zn _{0.17} Cd _{0.83}	-1.0	-2.3	-2.5	-4.3
ZnSe / ZnSe _{0.87} Te _{0.13}	Zn	-0.4	-1.9	-2.4	-5.0
	Se	-0.6	-1.9	-2.4	-5.0
	Se _{0.87} Te _{0.13}	-0.6	-1.9	-2.4	-5.0
	Zn	-0.4	-1.9	-2.4	-5.0
ZnSe / Zn _{0.85} Cd _{0.15} Se	Zn	-0.4	-2.0	-2.2	-5.0
	Se	-0.4	-2.0	-2.2	-5.2
	Se	-0.4	-2.0	-2.2	-4.9
	Zn _{0.85} Cd _{0.15}	-0.4	-2.0	-2.2	-5.0

TABLE IV. Energy-eigenvalues for the FISIM states (see text), B_{Ih} , B_{Il} , and B_{Is} , at the interface dominion of (001)-CdTe/CdSe_{0.15}Te_{0.85}, (001)-CdTe/Zn_{0.17}Cd_{0.83}Te, (001)ZnSe/ZnSe_{0.87}Te_{0.13}, and (001)-ZnSe/Zn_{0.85}Cd_{0.15}Se.

		Γ -point			X -point		
System	Atomic layer	B_{Ih}	B_{Il}	B_{Is}	B_{Ih}	B_{Il}	B_{Is}
CdTe/CdSe _{0.15} Te _{0.85}	Cd	-2.4	-2.5	-4.5	-2.6	-3.1	-4.6
	Te	-2.4	-2.5	-4.5	-2.6	-3.1	-4.6
	Se _{0.15} Te _{0.85}	-2.4	-2.5	-4.5	-2.4	-3.0	-4.6
	Cd	-2.4	-2.5	-4.5	-2.6	-3.0	-4.6
CdTe/Zn _{0.17} Cd _{0.83} Te	Cd	-2.5	-2.9	-4.6	-2.7	-3.2	-4.7
	Te	-2.5	-2.7	-4.5	-2.5	-3.0	-4.5
	Te	-2.5	-2.9	-4.5	-2.5	-2.9	-4.7
	Zn _{0.17} Cd _{0.83}	-2.5	-2.9	-4.7	-2.7	-3.2	-4.8
ZnSe/ZnSe _{0.87} Te _{0.13}	Zn	-2.0	-2.2	-5.1	-1.9	-2.4	-5.2
	Se	-2.0	-2.2	-5.2	-1.9	-2.4	-5.2
	Se _{0.87} Te _{0.13}	-2.0	-2.2	-5.2	-1.9	-2.4	-5.2
	Zn	-2.0	-2.2	-5.1	-1.9	-2.4	-5.2
ZnSe/Zn _{0.85} Cd _{0.15} Se	Zn	-2.0	-2.2	-5.1	-2.2	-2.4	-5.2
	Se	-2.0	-2.2	-5.1	-2.2	-2.4	-5.2
	Se	-2.0	-2.2	-5.1	-2.2	-2.4	-5.1
	Zn _{0.85} Cd _{0.15}	-2.0	-2.2	-5.1	-2.2	-2.4	-5.2

(001)-CdTe/CdSe_{.15}Te_{.85}

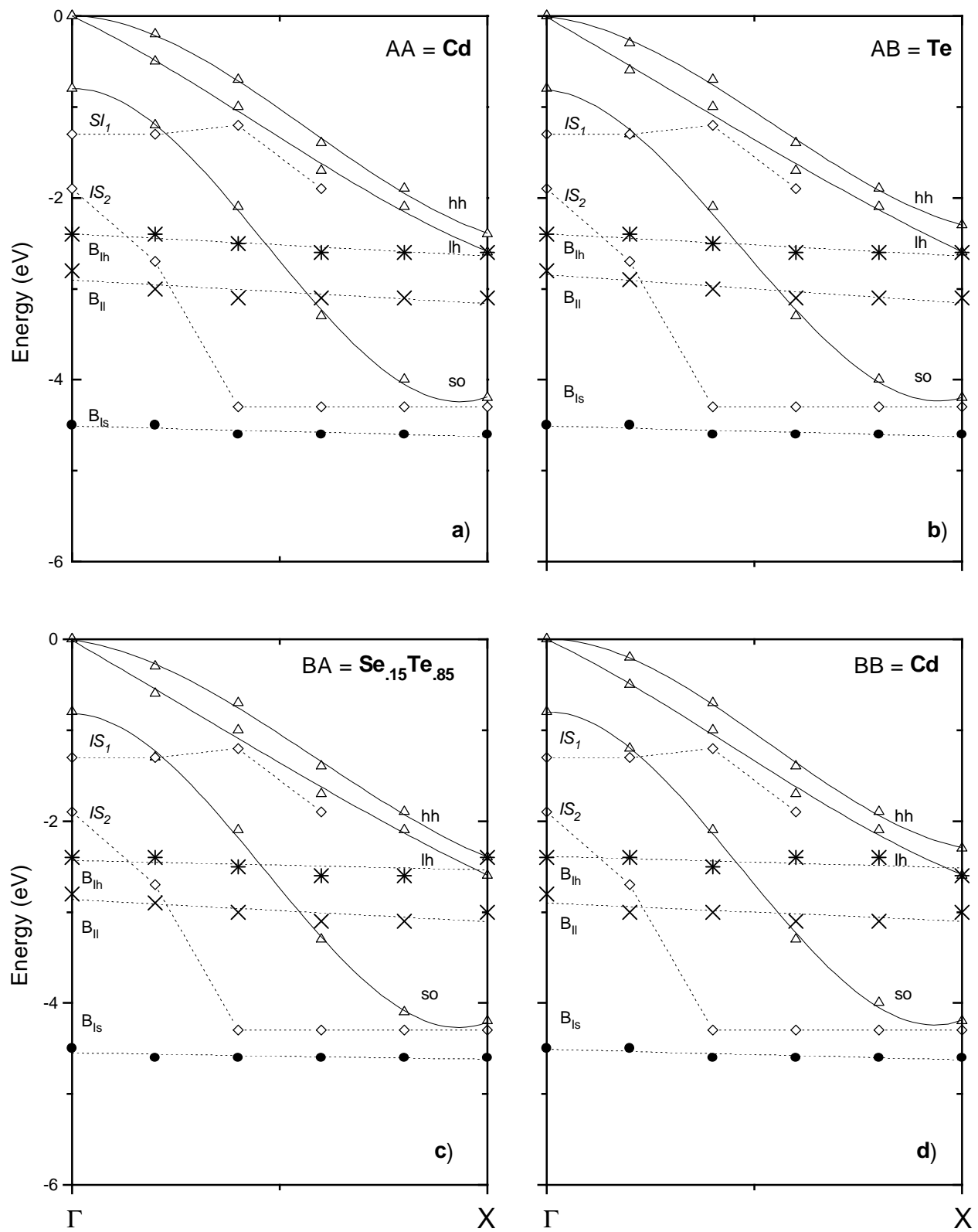


Fig. 1, Z. Phys. B, Olguin & Baquero

(001)-CdTe/ $\text{Zn}_{.17}\text{Cd}_{.83}\text{Te}$

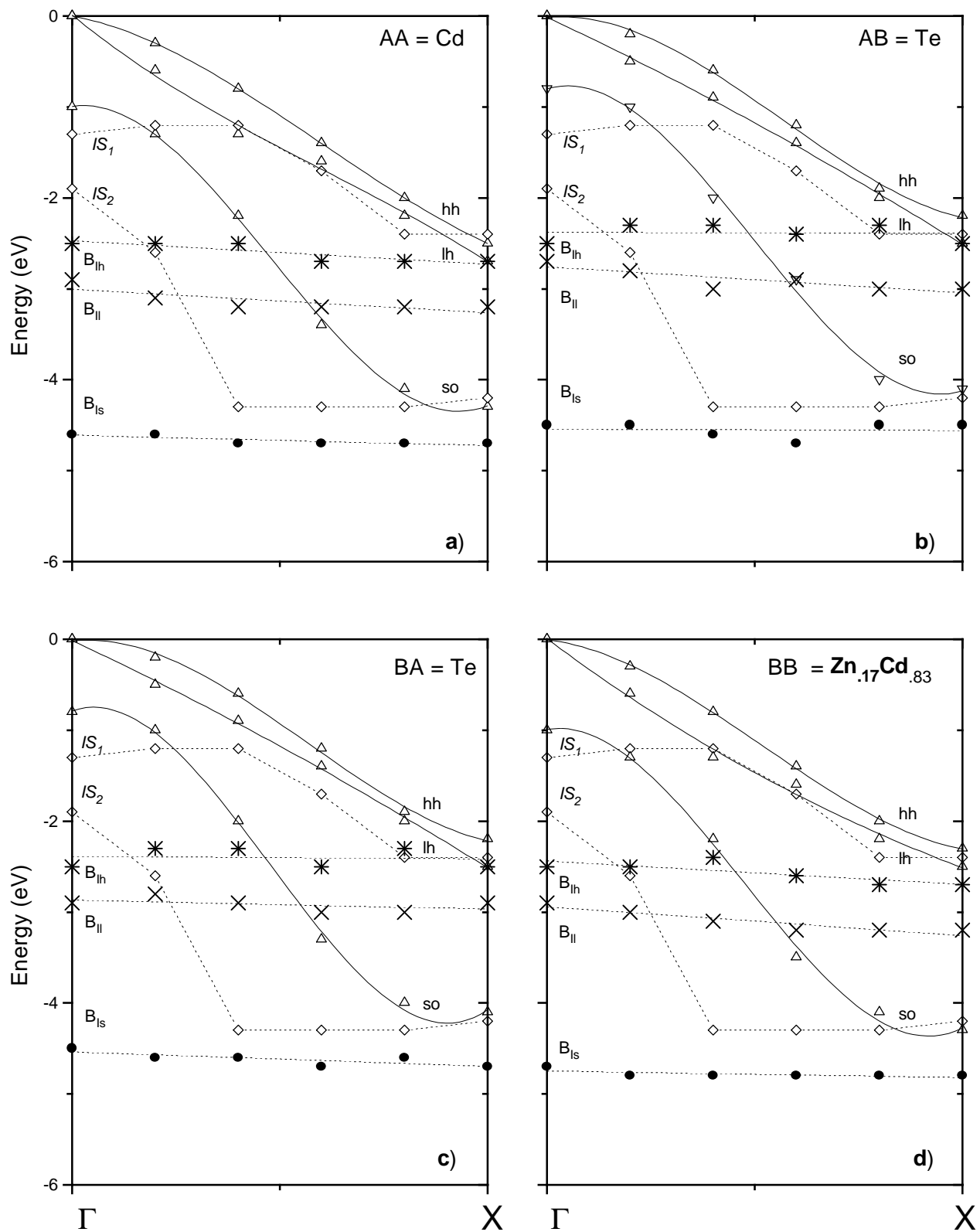


Fig. 2, Z. Phys B, Olguin & Baquero

(001)-ZnSe/ZnSe_{.87}Te_{.13}

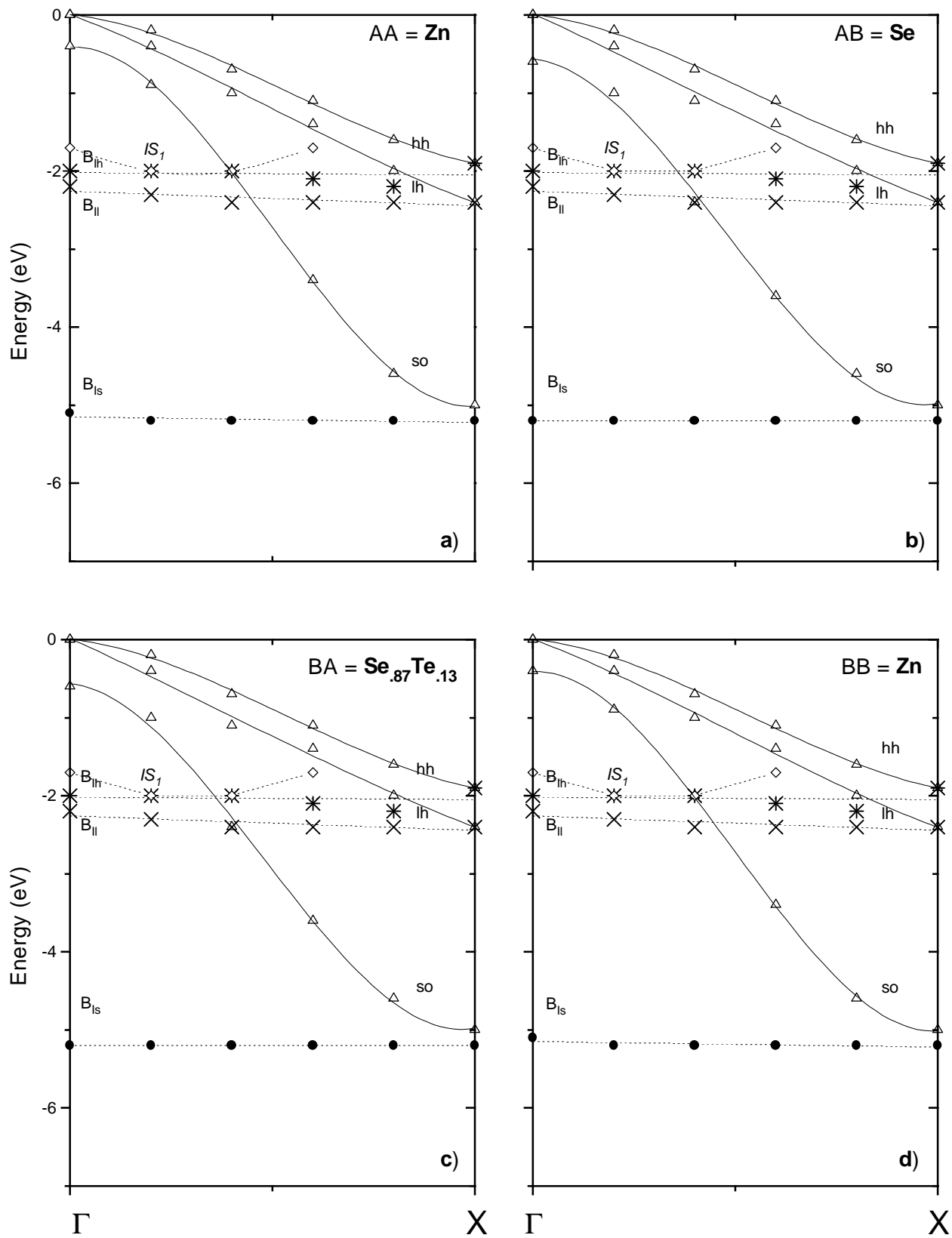


Fig. 3, Z. Phys. B, Olguin & Baquero

(001)- ZnSe/Zn_{.85}Cd_{.15}Se

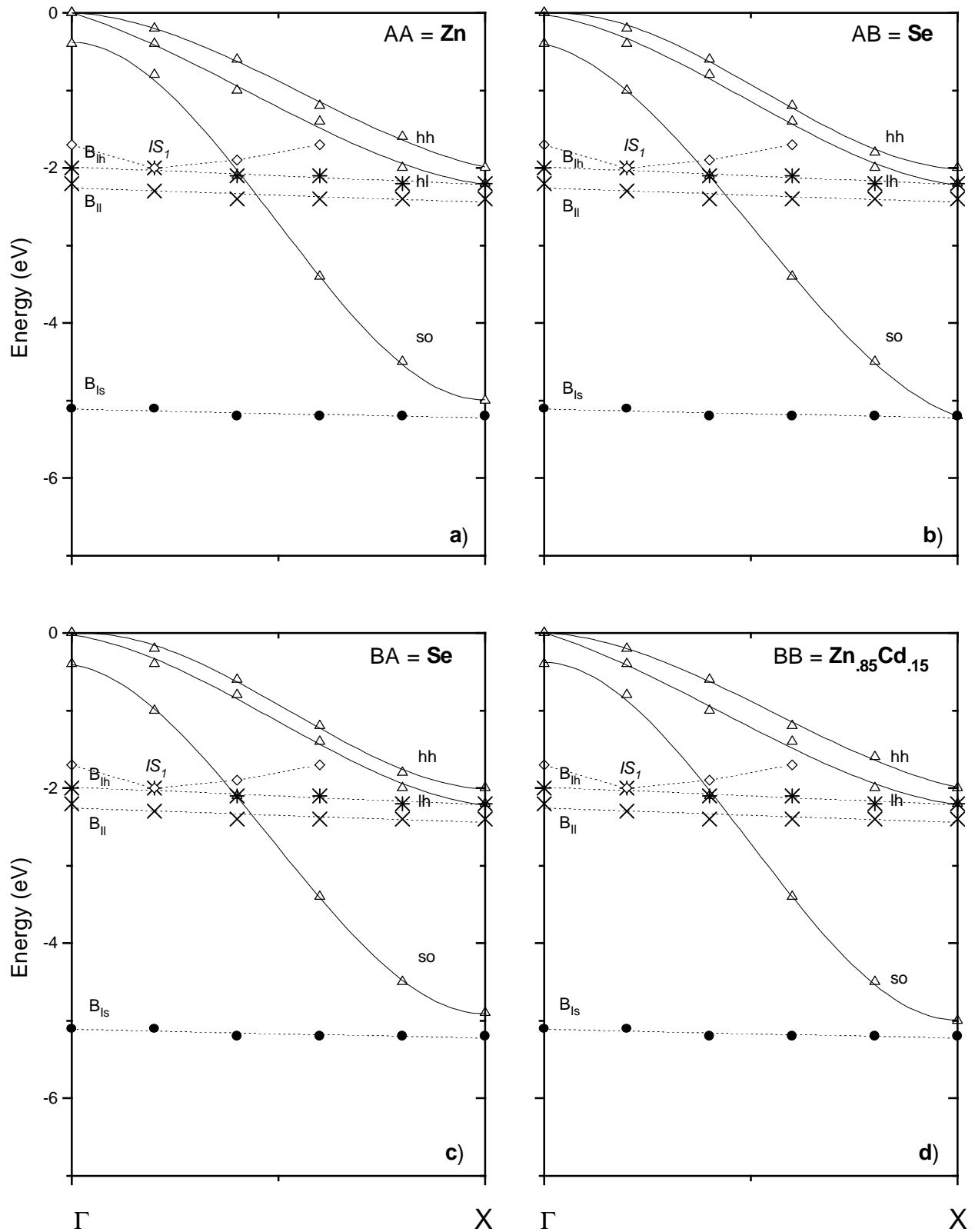


Fig. 4, Z. Phys. B, Olguin & Baquero